26th EPS Conf. on Contr. Fusion and Plasma Physics, Maastricht, 14 - 18 June 1999 ECA Vol.23J (1999) 669 - 672

Computation of Parallel Flow and Concomitant Electric Field in the Collision Dominated Edge of Tokamak Plasmas

A. Nicolai, A. Rogister

Forschungszentrum Jülich GmbH, Association EURATOM-KFA, 52425 Jülich, FRG

Introduction

The discovery of the L - H transition in divertor tokamaks has evoked considerable and widespread efforts to investigate improved confinement regimes.

In particular the ambipolarity and the parallel momentum equations of the revisited neoclassical theory [1] allow, by means of a simplified analytical solution, to estimate the normalized parallel speed and poloidal speeds, $g = \frac{B_\theta}{B_\phi}\frac{v_{||}}{v_T}$ and $h = \frac{v_\Theta}{v_T}$, respectively, as well as the radial electric field E_r. The crucial parameter of this theory $\Lambda_1 = \frac{q^2R^2N_i}{\chi_{||_i}}\frac{T_i'}{eB_t} = \frac{0.255}{\Omega_i\tau_i}\frac{q^2R^2}{rL_{T_i}}$, entering both equations, measures the ratio of the contributions arising from perpendicular viscosity to those from the parallel viscosity. (In the case of low collisionality the collision time τ_i should be replaced by the transit time $\frac{qR}{v_{th_i}}$ so that $\Lambda_1 \to 0.255\frac{\rho_{i_p}}{L_{T_i}}$, where ρ_{i_p} is the Larmor - radius in the poloidal magnetic field.) The equations also account for the friction with the neutral gas due to recycling and for neutral beam injection. They are solved numerically (1) to benchmark with a simplified analytical theory and (2) to explore the parameter space in regions where the simplified analytical theory is not valid[2].
However, the time independent theory resorting to prescribed profiles of the T_i, T_e, N_e cannot model the strongly time dependent L - H transition.
Therefore the time dependent ambipolarity and the time independent (modified) momentum equations, both given below, were investigated using the Crank - Nicholson difference scheme with a generalized upwind differencing in space and centered differences in time. The predictor - corrector code equation might be embedded in a transport code as it is needed for tracking the temperature evolution.

Ambipolarity and Momentum Equations

Introducing the definitions of the normalized speeds, $g = \frac{B_\theta}{B_\phi}\frac{v_{||}}{v_T}$, and $h = \frac{v_\Theta}{v_T}$, the ambipolarity constraint may be written in the dimensionless form [1,2]

$$\frac{\partial g}{\partial t} = -\frac{\kappa(r-r_s)+1}{\kappa pF(1+\frac{Q^2}{S^2})}\frac{\partial g}{\partial r} + 5\frac{\kappa(r-r_s)+1}{\kappa pF(1+\frac{Q^2}{S^2})}\frac{\partial h}{\partial r} + S_g \qquad (1)$$

The 'source' term S_g, given by $F(1+\frac{Q^2}{S^2})S_g = g^2 - (u_1+u_2)g + u_1u_2$, is nonlinear (quadratic) in g. The sum and the product of the normalized speeds u_1 and u_2 depend on the profile parameters κ, p, η, z (defined in the following) the neutral gas density, neutral beam injection power and on the velocities Q and S [1] (i. e. on h and Λ_1).

The ion temperature, ion density and Z_{eff} - profiles are assumed to have the radial dependences /1/

$$T = T_{i_s}[f(r)]^p \quad n = n_{i_s}[f(r)]^{\frac{p}{\eta}} \quad Z_{eff} = Z_{eff_s}[f(r)]^z$$

with $f(r) = 1 + \kappa(r - r_s)$, r_s is the radius of the last closed flux surface (LCFS). T_{i_s}, n_{i_s} and Z_{eff_s} are temperature, density and Z_{eff}, respectively, at this surface.

Combining the parallel momentum equation [1] with the ambipolarity equation we get the time independent equation

$$2\frac{\kappa(r - r_s) + 1}{\kappa p}\frac{\partial g}{\partial r} + h^2 - (v_1 + v_2)h + v_1 v_2 = 0 \tag{2}$$

The sum and the product of $v_{1,2}$ have a similar dependence as the sum and the product of $u_{1,2}$.

An artificial diffusive term $D_\epsilon = \epsilon\frac{\partial^2 g}{\partial r^2}$ is added to the right hand of equation (1). This term provides numerical stability and allows to impose a boundary condition at the inner radius r_{in} of the computational domain. (Furthermore, as in the time independent calculations, a pedestal boundary condition is imposed at the r_s.) In the case of upwind differencing of the convective terms ϵ can be reduced to $\epsilon = 10^{-8}$. In this case the term $|D_\epsilon|$ is much smaller then the other terms of equation (1) (in absolute value).

Analytic Solution and Asymptotic Behaviour

In the limit $\Lambda_1 \to 0$ and for h=-2.1 the most general solution

$$g_a(r) = \frac{c - u_2[1 + \kappa(r - r_s)]^{pc}H_1}{c - u_1[1 + \kappa(r - r_s)]^{pc}H_1}u_1 \approx 0.5\{(u_1 - u_2)tanh[0.5(u_1 - u_2)\xi] + (u_1 + u_2)\} \tag{3}$$

can be found analytically [1]. H_1 is computed from the boundary condition at r=r_s. c (<0) is defined as $c = u_1 - u_2$, ξ is given by $\xi = \frac{r - r_0}{L_{T_0}}$ with $L_{T_0} = \frac{\kappa(r_0 - r_s) + 1}{\kappa p}$. r_0 is the inflection point of $g_a(r)$. As asymptotic behaviour we get $g_a(-\infty) = u_1$ and $g_a(\infty) = u_2$. We note that r_0 is mainly determined by the boundary value $g(r_s)$.

Results

In the time dependent solutions presented here the assumption h= h_s = -2.1 is made because the time independent treatment in [2] shows that the deviation $|h - h_s|$ is small if the boundary condition (at the LCFS) $h_s = -2.1$ is chosen.

In all Figs. discussed below the time evolution of the radial electric field $E_r = (h - g - \frac{1}{\eta} - 1)E_0$ is displayed.

The sum $u_s = u_1 + u_2$, the product of $u_p = u_1 u_2$, the parameter Λ_1, the boundary and initial conditions determine the solution of the system. The initial condition is given by the linear dependence $g_i = zg_{in} + (1 - z)g_s$ with $z = \frac{r - r_s}{r_{in} - r_s}$.

To give two characteristic examples with and without transport barrier u_{p_1} = -10 is kept constant and u_s assumes the values -9 (with barrier) and 9 (without barrier). The reciprocal decaylength (negative) is $\kappa = -0.5\, cm^{-1}$.

Fig. 1 (u_{p_1}=-10, u_s = -9, u_1 = -10, u_2 = 1) and Fig. 2 (u_{p_1}=-10, u_s = 9 u_1 = -1, u_2 = 10) are devoted to the comparison of the time dependent numerical solution with the analytical theory which is valid for $|\Lambda_1| \to 0$. For the choice $|\Lambda_1| = 0.02$ and the boundary condition g_s=0.99 the radial field E_r starting with a linear dependence ($g_{in} = -9,\ g_s = 0.99$) relaxes almost exactly to the analytical solution [1,2], characterized by the hyperbolic tangent of equation (3).
The jump of the electric field, $E_{max} - E_{min} \approx 60\frac{kV}{m}$, and that of the parallel velocity, $v_{||,max} - v_{||,min} \approx 90\frac{km}{sec}$, are in reasonable agreement with reported values [1,2].

In Fig. 2 ($g_{in} = -1,\ g_s = 0.99$) E_r evolves to its analytical dependence which is now due to the boundary value $g_s = 0.99$ a small part of the curve of the hyperbolic tangent. We note that $g_s = 10$ would entail the 'full hyperbolic tangent'. However, as pointed out in [2], the justification of this boundary value is problematical. The variation of the electric field, $E_{max} - E_{min} \approx 5\frac{kV}{m}$, is comparatively small, i.e. there is no barrier.

In Figs. 3, 4 the deviations due to the large $|\Lambda_1| = 0.4$ are investigated. In Fig. 3 (u_{p_1}=-10, u_s = -9, u_1 = -10, u_2 = 1) the initial distribution which is the same as in Fig 1 ($g_{in} = -9,\ g_s = 0.99$), relaxes to a dependence with an overshoot beyond the asymptotic value. This value is the same as in Fig. 1. As a consequence the slope at $r = r_s$ is much steeper than in Fig. 1. Thus the time independent results in [2] are reproduced qualitatively.

In Fig. 4 (u_{p_1}=-10, $u_s = 9$ u_1 = -1, $u_2 = 10$) the relaxation from the initial distribution which is the same as in Fig. 3 ($g_{in} = -9,\ g_s = 0.99$) and differs strongly from the relaxed distribution, can be seen to happen essentially in 30 msec. After 100ms the distribution settles down to one similar to that in Fig. 2, however, with an overshoot as in Fig. 3.

Conclusions and Discussion

The time dependent solutions presented so far suffer from the fact that h(r,t) is assumed to be constant. In the case of the boundary condition h_s = -2.1 this may be a good assumption if $|\Lambda_1|$ is small. In view of the time independent solutions in [2] one can expect that for large $|\Lambda_1|$ quantitative deviations will occur (increase of the overshoot, oscillatory behaviour).

The unknown boundary conditions at r = r_s, introduce a strong uncertainty. Nevertheless, the computed electric fields and rotation velocities seem to be in reasonable agreement with reported values [1].

[1] A. Rogister, Physics of Plasmas 6, 200 (1999)
[2] A. Nicolai, Theory of Fusion Plasmas, Proceedings of the Joint Varenna - Lausanne International Workshop (1998)

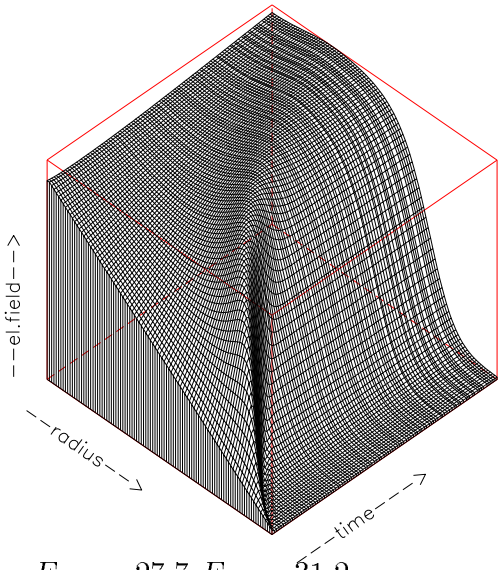

E_{min}=-27.7 E_{max}=31.2
Fig. 1

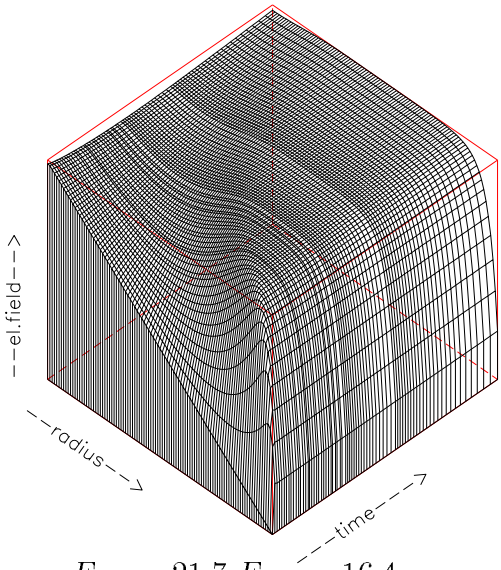

E_{min}=-21.7 E_{max}=-16.4
Fig. 2

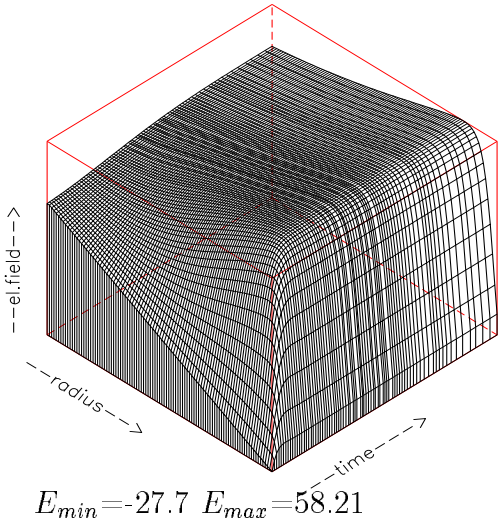

E_{min}=-27.7 E_{max}=58.21
Fig. 3

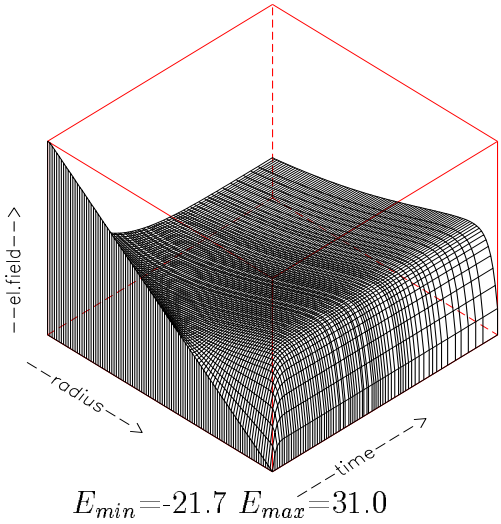

E_{min}=-21.7 E_{max}=31.0
Fig. 4

Evolution of the radial el. field E_r. Due to $|\Lambda_1| = 0.02$ (Figs. 1, 2) E_n evolves to its analytical dependence. Figs. 1, 3 belong to $u_s = -9$ and Figs. 2, 4 to $u_s = 9$. For $|\Lambda_1| = 0.4$ the analytical asymptotic values are retrieved (Figs. 3, 4), however, the radial dependence is characterized by an overshoot. The spatial extension is 5 cm and and the final time 100 ms. E_{max}, E_{min} are in kV/m.